Radiation Medicine and Protection 4 (2023) 204–213

Contents lists available at ScienceDirect

Radiation Medicine and Protection

journal homepage: www.radmp.org

Original article

Hexyl-pentynoic acid serves as a novel radiosensitizer for breast cancer by inhibiting UCHL3-dependent Rad51 deubiquitination

Zuchao Cai [a,b], David Lim [c,d], Beidi Jia [a], Guochao Liu [a], Wenwen Ding [a], Zhendong Wang [a], Zhujun Tian [a], Junxuan Peng [a], Fengmei Zhang [a], Chao Dong [a], Zhihui Feng [a,*]

[a] Department of Occupational Health and Occupational Medicine, School of Public Health, Cheeloo College of Medicine, Shandong University, Jinan 250012, China
[b] Stomatology Hospital, School of Stomatology, Zhejiang University School of Medicine, Zhejiang Provincial Clinical Research Center for Oral Diseases, Key Laboratory of Oral Biomedical Research of Zhejiang Province, Cancer Center of Zhejiang University, Hangzhou 310000, China
[c] Translational Health Research Institute, School of Health Sciences, Western Sydney University, Campbelltown, New South Wales, Australia
[d] College of Medicine and Public Health, Flinders University, Bedford Park, South Australia, Australia

ARTICLE INFO

Keywords:
2-hexyl-4-pentynoic acid
Radiosensitization
UCHL3
Rad51
Homologous recombination
Deubiquitination

ABSTRACT

Objective: To investigate the effects and underlying mechanism of 2-hexyl-4-pentynoic acid (HPTA), a derivative of valproic acid (VPA), on radiotherapy in breast cancer.

Methods: MCF7 cells and 7,12-dimethylbenz-[α]-anthracene (DMBA)-induced transformed human normal breast cells (MCF10A–DMBA cells) were irradiated with 8 Gy X-rays. For both cells there were four groups: control, valproic acid (VPA)/HPTA, IR, and VPA/HPTA+IR groups. MTT and clonogenic survival assays were performed to assess cell proliferation, and comet assay was performed to evaluate DNA damage. Protein expression of γH2AX, 53BP1, Rad51, and BRCA1 was examined *via* immunofluorescence and immunoblotting. Cycloheximide chase and ubiquitination experiments were conducted to determine Rad51 ubiquitination. *In vivo* experiments involved a rat model of DMBA-induced breast cancer, with four fractionated doses of 2 Gy. Tumor tissue pathological changes and γH2AX, Rad51, and UCHL3 expression levels were measured by hematoxylin-eosin staining, immunohistochemistry, and immunoblotting.

Results: Compared with the IR group, 15 μmol/L HPTA reduced the cell proliferation ability of irradiated MCF7 cells (t=2.16, P<0.05). The VPA/HPTA+IR group exhibited significantly increased DNA double-strand breaks relative to those in the IR group (VPA+IR *vs.* IR, t=13.37, P<0.05; HPTA+IR *vs.* IR, t=8.48, P<0.05). Immunofluorescence and immunoblotting experiments demonstrated that the VPA/HPTA+IR group displayed significantly increased cell foci formation, γH2AX and 53BP1 protein expression levels compared to the IR group [(γH2AX: VPA+IR *vs.* IR, t=8.88, P< 0.05; HPTA+IR *vs.* IR, t=8.90, P< 0.05), (53BP1, VPA+IR *vs.* IR, t=5.73, P< 0.05; HPTA+IR *vs.* IR, t=6.40, P< 0.05)]. Further, Rad51 expression was downregulated (VPA+IR *vs.* IR, t=3.12, P< 0.05; HPTA+IR *vs.* IR, t = 2.70, P<0.05), and Rad51 inhibition effectively counteracted HPTA-induced radiosensitization. Ubiquitination detection further verified that HPTA inhibits Rad51 expression *via* UCHL3-dependent Rad51 deubiquitination. *In vivo* study results showed that 20 mg/kg HPTA significantly enhanced the radiosensitivity of breast tumors in rats by inhibiting Rad51 expression.

Conclusions: HPTA is a highly effective radiosensitizer that enhances the radiotherapeutic efficacy of breast cancer treatment through UCHL3-dependent deubiquitination of Rad51.

1. Introduction

In recent years, breast cancer incidence in women has witnessed a rapid increase. Radiotherapy, a common treatment for breast cancer, has proven effective in improving post-mastectomy survival rates and reducing locoregional and ipsilateral recurrences.[1] However, ionizing radiation (IR) carries risks of severe adverse effects due to incidental dosage to the heart, lungs, and contralateral breast.[2] Therefore, the identification of a suitable radiosensitizer to enhance or sustain the therapeutic damage to malignant cells is of great interest.

Histone deacetylase inhibitors (HDACIs) have been explored as potential candidates for cancer therapy. Their potential mechanisms

* Corresponding author.
E-mail address: fengzhihui@sdu.edu.cn (Z. Feng).

https://doi.org/10.1016/j.radmp.2023.10.003
Received 28 June 2023; Received in revised form 13 September 2023; Accepted 10 October 2023
Available online 10 October 2023

include inducing cell cycle arrest (G_1 phase), inhibiting DNA synthesis, promoting apoptosis, destabilizing chromosome structures, and inducing autophagy.[3-5] The previous studies demonstrated that valproic acid (VPA), an HDACI used for epilepsy at therapeutic dosage of 50–100 mg/ml, increased the radiosensitivity of esophagus cancer,[6] lung cancer,[7] prostate cancer,[8] colon cancer,[9] osteosarcoma, and breast cancer cells.[10,11] At present, VPA derivatives are gaining attention, with some potentially showing similar anti-tumor effects to high-dose VPA. In particular, 2-hexyl-4-pentynoic acid (HPTA) reportedly exerts a strong inhibitory effect on HDAC activity in HeLa and cerebellar granule cells[12,13] (IC_{50} at 11–15 μmol/L HPTA *vs.* 348–448 μmol/L VPA). Although higher doses of HPTA[14] (1.25 mmol/kg, equivalent to 227.85 mg/kg; 450 μmol/L) have raised concerns pertaining to teratogenesis, lower doses have not been associated with toxicity or adverse events. HPTA, thus, seemed to hold promise as a sensitizer for breast cancer treatment.[15]

We previously found that VPA-induced radiosensitization is closely related to the impairment of DNA double-strand break (DSB) repair.[10] Error-free homologous recombination (HR) repair relies on a homologous template, such as a sister chromatid, with recombinase Rad51 playing a pivotal role in this process. VPA has been reported to sensitize breast cancer cells by inhibiting Rad51 protein expression by promoting RFWD3–Rad51 ubiquitination.[16] Both ubiquitination and deubiquitination are crucial for maintaining Rad51 levels. Recent studies have demonstrated the significance of ubiquitin carboxyl-terminal hydrolase L3 (UCHL3) in Rad51 deubiquitination. UCHL3 recruits Rad51 to DNA damage sites, promoting HR and rendering cancer cells resistant to DNA damage.[17] Another study investigated perifosine, an inhibitor of UCHL3, as a means to inhibit HR-mediated DNA DSB repair, highlighting the UCHL3–Rad51 deubiquitination pathway as a potential cancer therapy target.[18] Herein our objective was to explore HPTA as a radiosensitizer to IR in different *in vitro* and *in vivo* breast cancer models, with the aim to decipher the underlying mechanisms.

2. Materials and methods

2.1. Cells and administration

2.1.1. Cell culture

MCF7 and U2OS cell lines were purchased from American Type Culture Collection (ATCC, USA) and maintained in Dulbecco's modified Eagle's media with 10% fetal bovine serum (GIBCO, USA) and 1% penicillin–streptomycin (Sigma, USA). MCF10A cells were provided by Stem Cell Bank, Chinese Academy of Sciences, and cultured with Dulbecco's modified Eagle's media (DMEM)mixed with F-12 Ham (Sigma, USA) containing 5% horse serum (GIBCO, USA), 100 ng/ml cholera toxin (Sigma, USA), 20 ng/ml epidermal growth factor (Sigma, USA), 0.5 μg/ml hydrocortisone (Sigma, USA), 10 μg/ml human insulin (Sigma, USA), and 1% penicillin–streptomycin (Sigma, USA). HCC1937 cells were stably transfected with pcDNA3-wild-type BRCA1 (wtBRCA1) and vector control (pcDNA3). HCC1937 cells were cultured in RPMI 1640 media containing 10% fetal bovine serum (Gibco, USA) and 1% penicillin–streptomycin (Sigma, USA). All cells were confirmed to be free of mycoplasma contamination and maintained at 37°C with 5% CO_2.

2.1.2. Drug treatment and IR administration

IR was administered to both rats and cells using an X-ray irradiator (X-RAD225 OptiMAX, Pxi, USA) at 250 kVp and 12 mA, with a dose rate of 2.08 Gy/min. Cells were treated with VPA (Sigma, USA) or HPTA (TCI, Japan) 24 h prior to IR.

2.2. In vitro experiments

2.2.1. MTT assay

Cells were seeded in a 96-well plate at a density of 1×10^3 cells per well. They were treated with VPA (500 μmol/l) or HPTA (15, 30, 60 μmol/l) for 24 h, followed by exposure to 4 Gy X-ray. Subsequently, MTT solution (5 mg/ml, Sigma,USA) was added to the treated cells and incubated for 4 h at 37 °C. The medium was then replaced with dimethyl sulfoxide, and absorbance was measured at 490 nm using an enzyme immunoassay analyzer (Bio-Tek Synergy H1, USA).

2.2.2. Comet assay

Neutral and alkaline comet assay were performed using the Trevigen Comet Assay kit (4252-040-K, Trevigen, Gaithersburg, Maryland, USA). Cells were pretreated with 500 μmol/L VPA and 15 μmol/L HPTA for 24 h, followed by exposure to 8 Gy X-rays. Low-melting agar was combined with cell suspension at a ratio of 1:10 post-treatment, followed by immediate spreading onto comet slides. The slides were cooled for 30 min and then immersed in a lysis solution. Subsequently, they were immersed into cold alkaline unwinding solution for 1 h (for alkaline comet assay), followed by transfer into neutral or alkaline electrophoresis buffer at 21 V for 30 min at 4°C in the dark. Afterwards, the slides were washed twice with distilled water and 70% ethanol for 5 min, dried, and then stained with SYBR Gold (1:10,000, Trevigen, USA). The olive tail moment was utilized to represent cell-related DSBs.

2.2.3. Immunofluorescence

Cells were seeded in an eight-well chamber at a density of 3×10^4 cells per well. The detailed procedure has been described in our previous studies.[19,20] Cells were treated with 500 μmol/l VPA and 15 μmol/l HPTA for 24 h, followed by exposure to 8 Gy X-rays. For immunoblotting, primary antibodies specific to various proteins were employed, including γH2AX (1:500; EMD Millipore, Germany), 53BP1 (1:1,000; Gene Tex, USA), Rad51 (1:100; Santa Cruz, USA), and BRCA1 (1:100; Santa Cruz, USA). The secondary antibodies included Alexa Fluor 594 goat anti-mouse IgG (H+L) (1:300; Molecular Probes, Germany) and Alexa Fluor 488 chicken anti-rabbit IgG (H+L) (1:300; Molecular Probes, Germany). Images were captured using a fluorescence microscope (IX71+DP73, Olympus).

2.2.4. Immunoblotting

Immunoblotting was performed as previously reported.[19] Cells were treated with 500 μmol/l VPA and 15 μmol/l HPTA for 24 h, followed by exposure to 8 Gy X-rays. Whole-cell lysates were collected 6 h after IR. The primary antibodies used included γH2AX (1:500; EMD Millipore, Germany), 53BP1 (1:1,000; Gene Tex, USA), BRCA1 (1:200; Santa Cruz, USA), BRCA1 (1:250; Calbiochem, Germany), Rad51 (1:200; Santa Cruz, USA), Rad51 (1:2,500; Calbiochem, Germany), Ku70 (1:200; Santa Cruz, USA), Ku80 (1:200; Santa Cruz, USA), DNA-dependent protein kinase catalytic subunit (DNA-PKcs, 1:5,000; Abcam, England), ubiquitin (1:1,000; Cell Signaling Technology, USA), UCHL3 (1:1,000; Proteintech, USA), and GAPDH (1:2,000, ZSGB-BIO, China). The secondary antibodies used included goat anti-mouse IgG (H+L) (1:5,000, Thermo Fisher, USA) and goat anti-rabbit IgG (H+L) (1:5,000, Thermo Fisher, USA).

2.2.5. DSB assay

For the HR assay, we utilized MCF7 cells expressing a recombination substrate of the pDR-GFP reporter. This allowed us to determine the number of GFP-positive cells in the treated cells for analyzing spontaneous HR frequency using flow cytometry according to the method in references 10, 11. For the nonhomologous end-joining (NHEJ) assay, we utilized U2OS cells expressing an end-joining reporter (EJ5-GFP). This facilitated the determination of the number of GFP-positive cells in the treated cells for analyzing spontaneous NHEJ frequency using flow cytometry according to the method in reference 21.

2.2.6. BrdU incorporation for cell cycle analysis

For cell cycle analysis, 10 μmol/L BrdU (Sigma, USA) was immediately added to the treated cells for 30 min before harvesting, followed by fixation in 70% ethanol at −20°C overnight. Afterwards, cells were incubated with 0.4 mg/mL pepsin (Sigma, USA) in 2 mol/L HCL and

neutralized with 0.1 mol/L sodium borate. Subsequently, cells were incubated with the primary antibody anti-BrdU (BD, USA) and the secondary antibody Alexa Fluor-594 goat anti-mouse IgG (Molecular Probes, Germany). Nuclei were stained with DAPI (Sigma, USA). The filtered cells were then subjected to cell cycle analysis using flow cytometry.

2.2.7. Real-time quantitative reverse transcriptase PCR (qRT-PCR)

Genes with notable changes were identified through RNA sequencing using forward and reverse sequencing primers (Sangon Biotech, China). Primer specificity was verified using NCBI. Detailed protocols have been described in our earlier study.[22] MCF7 cells without any treatment served as control, and target gene expression in each group was compared. [$^{\Delta\Delta}$Ct = experimental group; $^{\Delta}$Ct = control group $^{\Delta}$Ct. $^{\Delta}$Ct = (average Ct of the target gene of the control sample− average Ct of the control sample GAPDH)]

Primers and their sequences are listed in Supplementary Table 1.

2.2.8. Clonogenic survival assay

Cells were seeded in P60 dishes and treated with 500 μmol/L VPA and 15 μmol/L HPTA for 24 h, followed by exposure to IR (2, 4, 6 Gy). They were cultured for approximately 2 w until visible colonies formed. At the endpoint, cells were fixed with ethanol and stained with 0.1 % crystal violet in 20 % methanol for 30 min, as previously reported.[15,23] The number of cell colonies were counted, and cell survival fraction calculated as follow: Cell survival fraction = (number of clones/seeded cells) / plating efficiency. These experiments were performed in triplicate.

2.3. In vivo experiments

2.3.1. Animal keeping and breast cancer model establishment

Female Sprague-Dawley (SD) rats were purchased from Pengyue Laboratory Animal Co. Ltd. Jinan, China. Detailed protocols have been described in our previous study.[10] All rats were housed in a specific pathogen-free environment at (23 ± 1)°C, with a daily light cycle of 12 h. They were provided *ad libitum* access to fresh food and water throughout the experiment. Animal care was conducted in accordance with relevant Chinese laws and guidelines for experimentation and scientific purposes. Breast tumors were induced in 50-d-old female SD rats weighing (150 ± 15) g (n = 60) through a single administration of 20 mg/ml 7,12-dimethylbenz-[α]-anthracene (DMBA, Sigma, USA) dissolved in sesame oil *via* oral gavage. The animals were palpated twice weekly for tumors.

At 50 d after gavage, rats with appropriate tumor size and location were selected for grouping (n = 6 in each group) and further investigation. Tumor size in each group was recorded and measured using a vernier caliper. Tumor volume was calculated as: $V = L \times W^2 \times 0.5$.

2.3.2. Hematoxylin-eosin and immunohistochemical staining

Hematoxylin-eosin and immunohistochemical staining was performed according to Reference 22. The primary antibodies used were γH2AX (1:500, EMD Millipore, Germany), Rad51 (1:500; Calbiochem, Germany), and BrdU (1:50, BD, USA), and the secondary antibodies used were biotinylated goat anti-mouse IgG (1:300, Vector, Germany) and biotinylated goat anti-rat IgG (1:300, Vector, Germany). Integrated optical density of γH2AX and Rad51 immunohistochemical staining was quantified with Image-Pro Plus (Media Cybernetics).

2.3.3. Chemical carcinogen-induced rat breast cancer-derived primary cells

The detailed procedure has been described elsewhere.[24] After breast cancer model establishment, SD rats were anesthetized using chloral hydrate, and breast cancer tissues were obtained in a sterile manner. These tissues were excised into small pieces (2 mm × 2 mm) and placed on coated dishes for primary cell culture. Cells from the second and third passages were used for immunofluorescence analyses of γH2AX and 53BP1.

2.3.4. Immunoprecipitation

Whole-cell lysate was mixed with Rad51 antibody (1 μg/mg protein lysate; Proteintech, USA) at 4°C for 2–3 h; protein A-Sepharose beads were added to this mixture, followed by incubation at 4°C overnight. The mixture was washed 4 times, denatured at 95°C for 5 min, and immunoblotting was then performed using standard protocols.

2.3.5. siRNA transfection

MCF7 cells were transfected with siRNAs (40 nmol/L final concentration) using lipofectamine 2000, as per manufacturer instructions (Sangon Biotech, Shanghai). siRNAs used in this study are listed in Supplementary Table 2.

2.4. Statistical analysis

Values represent mean ± standard deviation for the groups. Data were analyzed using independent sample t-test and normalized by Bonferroni post hoc test using SPSS for Windows v23.0 (Armonk, NY: IBM Corp; licensed to Shandong University). The P value < 0.05 indicated statistically significant differences.

3. Results

3.1. Low concentration of HPTA increases radiosensitization of tumor cells

Our previous study demonstrated that 500 μmol/L VPA inhibits breast cancer cell proliferation and increases cell sensitivity to radiation,[11] whether HPTA exerts a similar effect on breast cancer cells was firstly investigated in this study. MTT experiments were replicated using HPTA and MCF7 cells. We evaluated three concentrations of HPTA (15, 30, and 60 μmol/L) against 500 μmol/L VPA (as positive control), and cells were subjected to 4 Gy. As expected, we observed that cell proliferation in the HPTA-treatment groups was inhibited after IR ($P<0.01$, Fig. 1A). However, relative to the positive control, there were no statistically significant differences between the three different concentrations of HPTA (*ns*, $P> 0.05$, Fig. 1A), indicating that HPTA at a low concentration (15 μmol/L) possesses similar radiosensitizing effect as 500 μmol/L VPA. The results of clonogenic assay with MCF7 cells also indicated that 15 μmol/L HPTA exerts similar radiosensitizing effects *in vitro* as VPA (Fig. 1B, S1B). Consequently, 15 μmol/L HPTA was used for subsequent experiments.

Next, comet assays were performed to examine whether the lower concentration of HPTA could induce DSBs after IR in MCF7 cells. Neutral comet assay results revealed an increase in DSB levels in the HPTA-treatment group at 0, 30, and 120 min after IR exposure compared to DSB levels in the control group ($P < 0.01$; Fig. 1C). Alkaline comet assay results corroborated these findings (Fig. S1C). Furthermore, the formation of γH2AX and 53BP1 foci were assessed in MCF7 cells after IR exposure by immunofluorescence. The proportion of MCF7 cells with γH2AX or 53BP1 foci formation showed a significant increase at 6 h post-IR (81.37% and 87.34% respectively; Fig. 1D). HPTA treatment further augmented these percentages to 97.50% (γH2AX) and 98.21% (53BP1) ($P<0.01$; Fig. 1D). At 24 h post-IR, γH2AX and 53BP1 foci remained significantly more abundant in the HPTA-treated group as compared with that in the control group ($P<0.01$). Immunoblotting findings indicated an increase in γH2AX and 53BP1 levels after IR exposure, with further increases in the HPTA-treated group ($P<0.01$), consistent with the results obtained for the VPA-treated positive control group (Fig. 1E).

Subsequently, these findings were evaluated using the environmental carcinogen DMBA to induce transformation in MCF10A cells (MCF10A–DMBA cells). As anticipated, HPTA treatment increased IR-induced DNA damage in MCF10A–DMBA cells, resembling the effects seen with VPA (Figs. S1D–S1F).

To summarize, our data demonstrated that 15 μmol/L HPTA enhances radiosensitization in breast cancer cells, similar to the effects of 500 μmol/L VPA.

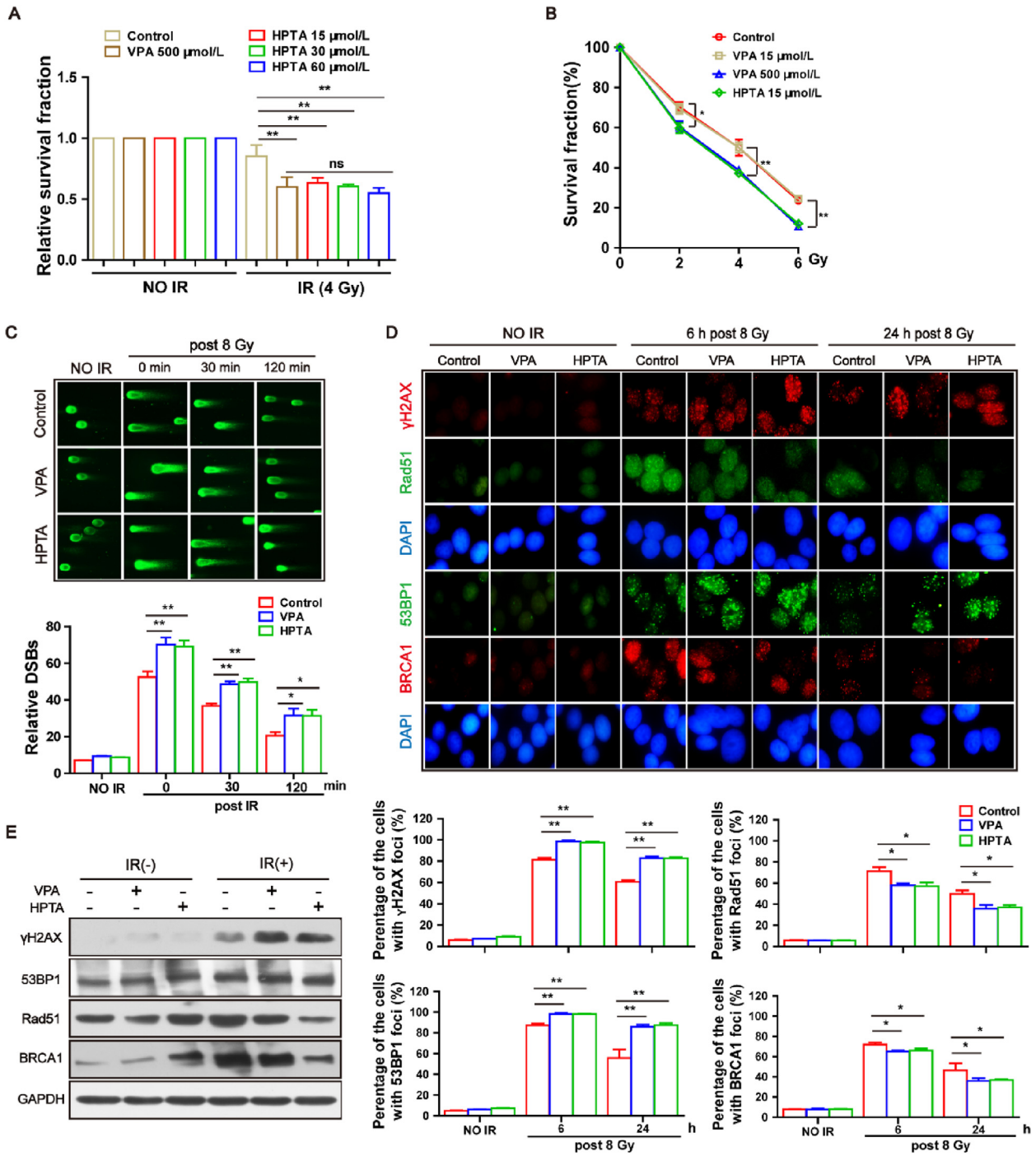

Fig. 1. Low 2-hexyl-4-pentynoic acid (HPTA) concentration enhances radiosensitization in tumor cells. A. MTT assay were used to detect growth of MCF7 cells treated with valproic acid (VPA) and 2-hexyl-4-pentynoic acid (HPTA) and exposed to 4 Gy ionizing radiation (IR). B. Clonogenic survival assay were used to detect survival fraction (%) of MCF7 cells treated with VPA and HPTA and different doses of IR. Cells were treated with VPA or HPTA for 24 h before IR exposure. C. Neutral comet assay were used to assess 8 Gy-induced DNA double-strand breaks (DSBs) in MCF7 cells, and assessment of relative DSBs. D. γH2AX, 53BP1, Rad51, and BRCA1 foci formation in MCF7 cells treated with 500 μmol/L VPA and 15 μmol/L HPTA after exposure to 8 Gy. Images depict γH2AX, 53BP1, Rad51, and BRCA1 foci formation before exposure to 8 Gy at 6 h and 24 h after exposure to 8 Gy. DAPI was used for nuclei staining. Percentage of γH2AX, 53BP1, Rad51, and BRCA1 foci formation was evaluated. Cells containing at least 20 γH2AX or 53BP1 foci per cell and at least 10 Rad51 or BRCA1 foci per cell were regarded as positive cells. E. Immunoblotting was used to detect γH2AX, 53BP1, Rad51, and BRCA1 levels in MCF7 cells. Each data point in the graph represents data collected from three independent experiments (mean ± SD). *P* was calculated by *t*-test (**P*<0.05, ***P*< 0.01).

3.2. Low-dose HPTA inhibits HR function for repairing IR-induced DNA DSBs

To determine whether the radiosensitizing effect mediated by HPTA is associated with DNA repair function, HR frequency was evaluated. Using MCF7 cells expressing the pDR-GFP recombination reporter, HR frequency assay was performed through using flow cytometry after introducing I-SceI-induced DSBs (Fig. S2A). HR frequency was observed to decrease in cells treated with 15 μmol/L HPTA by 42.88% as compared to that in cells without HPTA treatment (*P*<0.01; Fig. 2A). Furthermore,

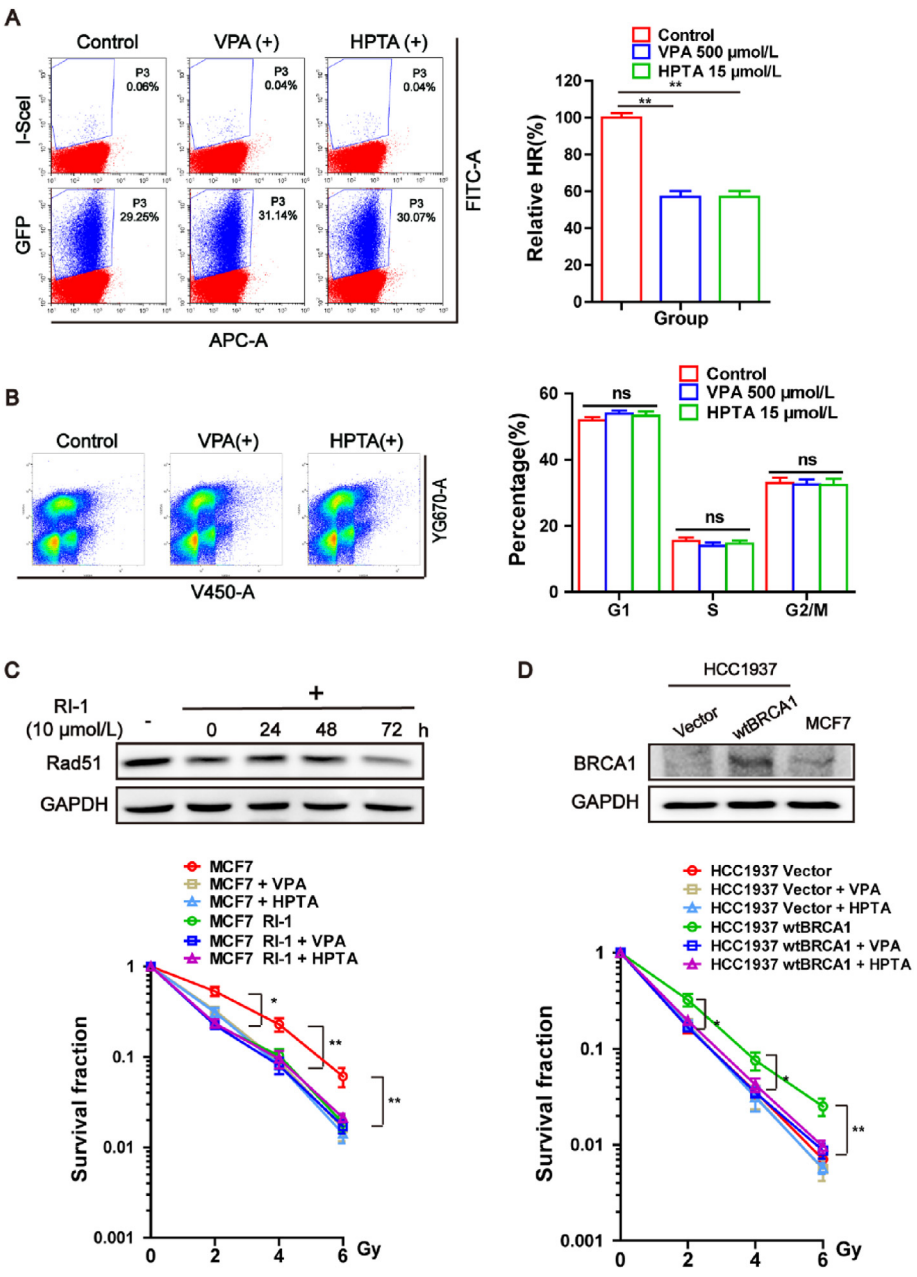

Fig. 2. Low 2-hexyl-4-pentynoic acid (HPTA) concentration inhibits homologous recombination (HR) function for repairing ionizing radiation (IR)-induced DNA double-strand breaks (DSBs). A. MCF7 cells expressing pDR–GFP were transfected with I-SceI or GFP plasmids and then treated with 15 μmol/L HPTA for 24 h. GFP served as a positive control to assess transfection efficiency. Images show HR frequency in HPTA-treated cells, as measured by flow cytometry. B. Cell cycle profiling of MCF7 cells pretreated with HPTA for 24 h. C. MCF7 cells were treated with 10 mmol/L RI-1 for 24 h, and Rad51 protein expression was detected by immunoblotting. Colony formation assay: MCF7 cell survival was assessed after different treatments. Survival fraction of different groups is shown. D. Colony formation assay: Survival of HCC1937 cells with and without BRCA1 expression was assessed after different treatments. Survival fraction of different groups is shown. Each data point in the graph represents data collected from three independent experiments (mean ± SD). *P* was calculated by *t*-test (**P* < 0.05, ***P* < 0.01).

cell cycle analyses indicated that HPTA did not cause cell accumulation in the S phase ($P>0.05$; Fig. 2B), indicating that the reduction in HR function was not correlated with cell cycle. Thus, our data demonstrated that low HPTA concentration effectively inhibits HR repair activity.

The recombinase Rad51, a key component of the mechanism underlying HR, was the next target of investigation to determine whether HPTA affects its activity. Immunofluorescence assay findings revealed that at 6 h after IR, the percentage of cells with Rad51 foci in the negative control group was 71.22% and was reduced by 14.04% ($P<0.01$) in the HPTA-treated group (Fig. 1D). At 24 h after IR, as DNA repair was gradually completed, the percentage of cells with Rad51 foci decreased. However, relative to the negative control group (49.96%), the HPTA-treated group still exhibited a significant reduction in Rad51 foci formation (13.05%, $P<0.01$). In addition, we found that the changes in another HR-associated protein, BRCA1, foci formation were similar to those observed for Rad51 (Fig. 1D). These findings were consistent with the changes in Rad51 and BRCA1 protein levels observed through immunoblotting ($P<0.01$; Fig. 1E) and at the transcriptional level ($P<0.01$; Fig. S2B). In MCF10A–DMBA cells, both Rad51 and BRCA1 proteins were also significantly inhibited in the HPTA-treated group in response to DNA damage ($P<0.05$; Figs. S1E and S1F).

To investigate whether the radiosensitizing effect mediated by VPA is Rad51 dependent, RI-1 was employed, an inhibitor of Rad51, to suppress Rad51 activity in MCF7 cells.[25] Immunoblotting analysis indicated that 10 mmol/l RI-1 significantly inhibited Rad51 protein expression (Fig. 2C). Rad51 inhibition led to increased sensitivity to IR, thus compromising the radiosensitizing effect of HPTA (Fig. 2C, S2C). We also confirmed that BRCA1 had a similar effect as Rad51 using an isogenic paired cell line (HCC1937) with and without BRCA1 expression, suggesting that the radiosensitizing effect of HPTA is BRCA1 dependent (Fig. 2D, S2D). These findings indicated that HPTA impairs Rad51 and BRCA1 activity upon IR exposure, further confirming that HPTA-mediated radiosensitization of tumor cells is associated with the inhibition of HR.

Next, to investigate the possibility that HPTA influences NHEJ repair, U2OS cells was used by expressing the EJ5-GFP reporter to measure

NHEJ frequency[21,26] using flow cytometry after introducing I-SceI-induced DSBs (Fig. S2E). NHEJ frequency was found to decrease in cells treated with 15 μmol/L HPTA by 19.48 % as compared to that in cells without HPTA treatment ($P<0.05$; Fig. S2E), indicating that HPTA disrupts NHEJ function. Immunoblotting assay was performed with MCF7 cells to detect the major NHEJ-associated proteins in our cell models, and the results showed that after 8 Gy, no significant changes in DNA-PKcs, Ku70, and Ku80 proteins were observed ($P>0.05$; Fig. S2F). Considering that the reduction in NHEJ efficiency induced by HPTA (19.48 %) was not as obvious as that observed in HR (42.88%), we believe that the effect of HPTA on HR is more significant than that on NHEJ.

3.3. HPTA-induced radiosensitization involves changes in Rad51 stability and ubiquitination

To investigate whether changes in Rad51 and BRCA1 protein levels are associated with protein stability, cycloheximide (CHX) chase assay was performed. (Fig. 3A, S3). After IR exposure, Rad51 protein levels in the control group decreased to 54.45% and 36.61% at 4 h and 8 h after CHX treatment, respectively. In contrast, in the HPTA-treated group, Rad51 protein levels decreased to 55.29% and 31.39% only at 2 h and 4 h after CHX treatment, respectively. These findings suggested that the half-life of Rad51 protein in the HPTA-treated group was shortened by 2 h, indicating that HPTA can inhibit Rad51 protein stability. The change

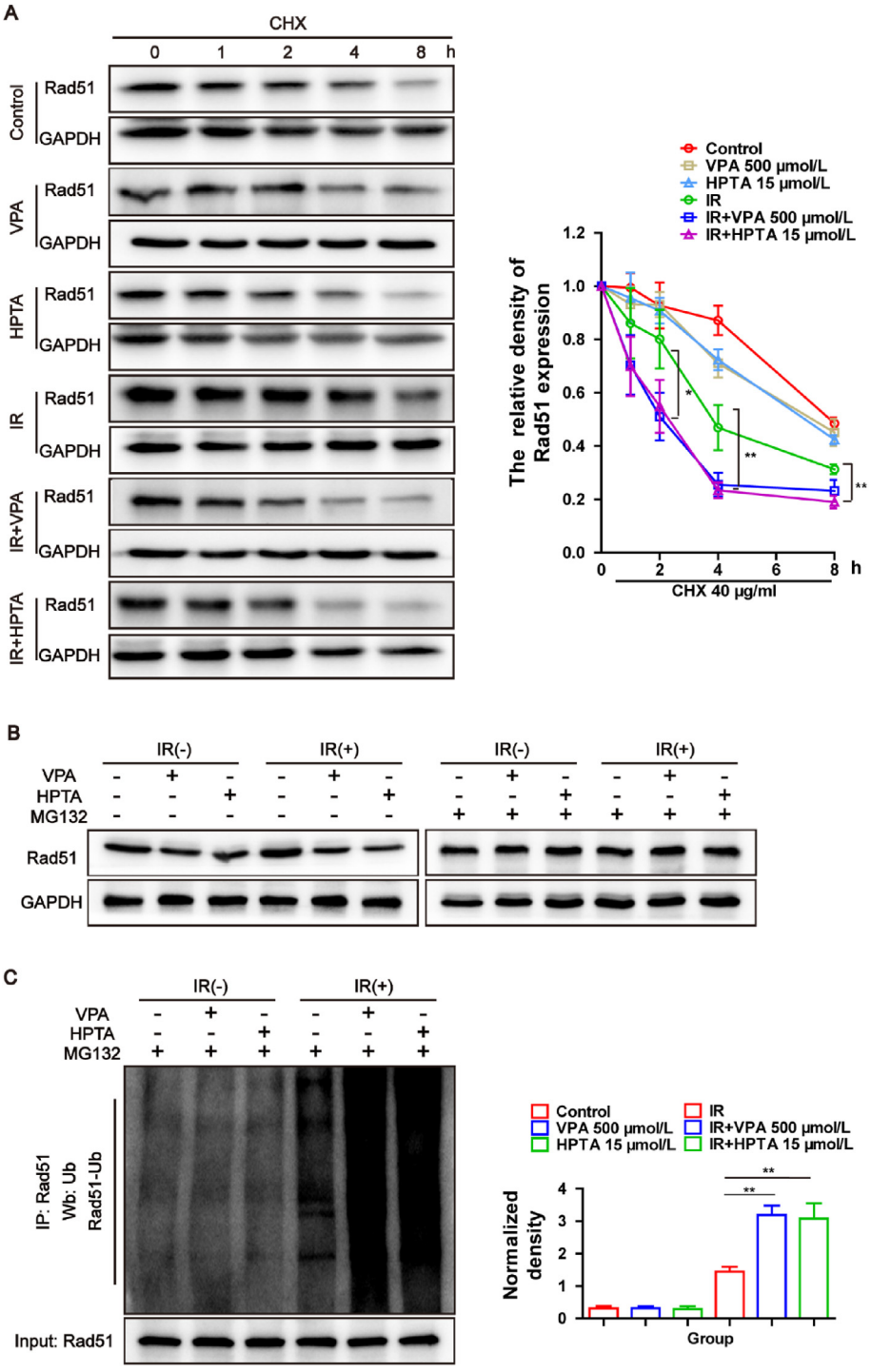

Fig. 3. 2-Hexyl-4-pentynoic acid (HPTA) affects Rad51 stability and ubiquitination during the radiosensitization process. A. Rad51 protein changes were detected by immunoblotting after treating MCF7 cells with cycloheximide (CHX, 40 μg/ml) for 0, 1, 2, 4, and 8 h. MCF7 cells were treated with 40 mmol/l MG132 at 6 h before harvesting whole cell extracts. B. Rad51 protein expression was detected by immunoblotting. C. Rad51 ubiquitination was detected by immunoprecipitation. Protein band intensities were quantified by ImageJ. Each data point in the graph represents data collected from three independent experiments (mean ± SD). *$P<0.05$, **$P<0.01$.

observed in BRCA1 protein after CHX treatment paralleled that of Rad51 (Fig. S3).

Given that Rad51 protein stability was found to be related to HPTA-mediated radiosensitization, we explored its ubiquitination status in MCF7 cells. Cells were treated with the 26S proteasome inhibitor MG132 for 6 h before harvesting. We found that MG132 restored the effects of HPTA on Rad51 protein levels (Fig. 3B) and that Rad51 ubiquitination was increased by the combined treatment compared to IR alone ($P<0.01$, Fig. 3C). These findings suggested that HPTA exerts its radiosensitizing effect of breast cancer cells by regulating Rad51 ubiquitination.

3.4. UCHL3–Rad51 deubiquitination pathway is involved in HPTA-mediated radiosensitizing effect

UCHL3 has been found to directly interact and deubiquitinate Rad51.[27] Thus, herein we investigated the effect of UCHL3 using MCF7 cells. Immunoblotting analysis indicated that the combined treatment significantly reduced UCHL3 protein levels compared to IR alone (Fig. 4A). Furthermore, co-immunoprecipitation experiments showed that both UCHL3 and Rad51 were part of a protein complex (Fig. 4B), suggesting an association between these proteins. To validate our results, we established an MCF7 cell line with siRNA-mediated depletion of UCHL3 (Fig. 4C). After downregulating UCHL3 expression in MCF7 cells, no significant differences were found in Rad51 protein levels in the IR alone and combined treatment groups (Fig. 4C, S4); besides, the increased ubiquitination level of Rad51 was abolished ($P>0.05$, Fig. 4D). Thus, we believe that UCHL3-dependent Rad51 deubiquitination is involved in HPTA-mediated radiosensitizing effect.

3.5. HPTA exhibits radiosensitizing effects by targeting the UCHL3–Rad51 deubiquitination pathway in DMBA-induced breast cancer in vivo

To determine whether HPTA exhibits a radiosensitizing effect *in vivo*, a rat model of DMBA-induced breast cancer was used, which has been previously described and utilized in related studies (Figs. S5A and S5B).[24] 4 fractionated doses of 2 Gy, based on previous studies, were administered.[28] HPTA (20 mg/kg) was administered before, during, and after IR exposure (Fig. S5C). All rats survived throughout the 32 d observation period. In comparison with the IR alone group, HTPA pretreatment significantly reduced tumor volume ($P<0.05$, Fig. 5A), indicating that HPTA exhibits radiosensitizing effects *in vivo*. 10 d after treatment, tumors were excised under general anesthesia (Fig. 5A); tumor size in the combined treatment group was smaller than that in the IR alone group. Hematoxylin-eosin staining results revealed that IR exposure led to vacuole structure formation in breast cancer tissues, and large damaged areas and cells were observed in the combined treatment group (Fig. 5B). These results demonstrated that 20 mg/kg HPTA can effectively sensitize breast cancer to IR treatment.

Whether HPTA influences DNA damage and repair proteins *in vivo* were explored next. After the administration of both HPTA and IR, DSBs detected by γH2AX were enhanced through immunohistochemistry ($P<0.01$; Fig. 5C), although no statistically significant change was

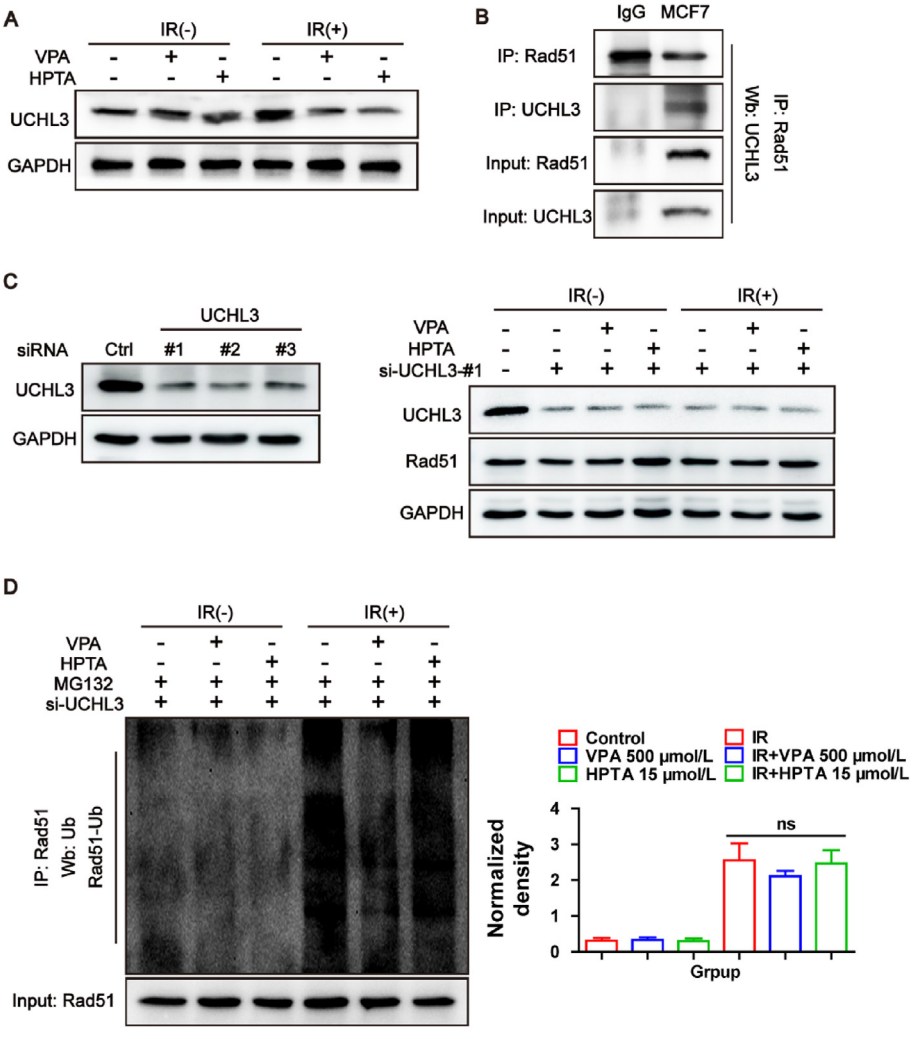

Fig. 4. Ubiquitin carboxyl-terminal hydrolase L3 (UCHL3)–Rad51 deubiquitination pathway is involved in HPTA-mediated radiosensitizing effect. A. UCHL3 protein expression level in MCF7 cells was detected by immunoblotting. B. Interaction between UCHL3 and Rad51 proteins was assessed through immunoblotting using protein beads containing Rad51 antibody. C. siRNA was used to deplete UCHL3 in MCF7 cells, and Rad51 expression was detected by immunoblotting. D. Rad51 ubiquitination in MCF7 cells after UCHL3 depletion was detected through immunoblotting. Protein band intensities were quantified by ImageJ. Each data point in the graph represents data collected from three independent experiments (mean ± SD). $^{*}P<0.05$, $^{**}P<0.01$.

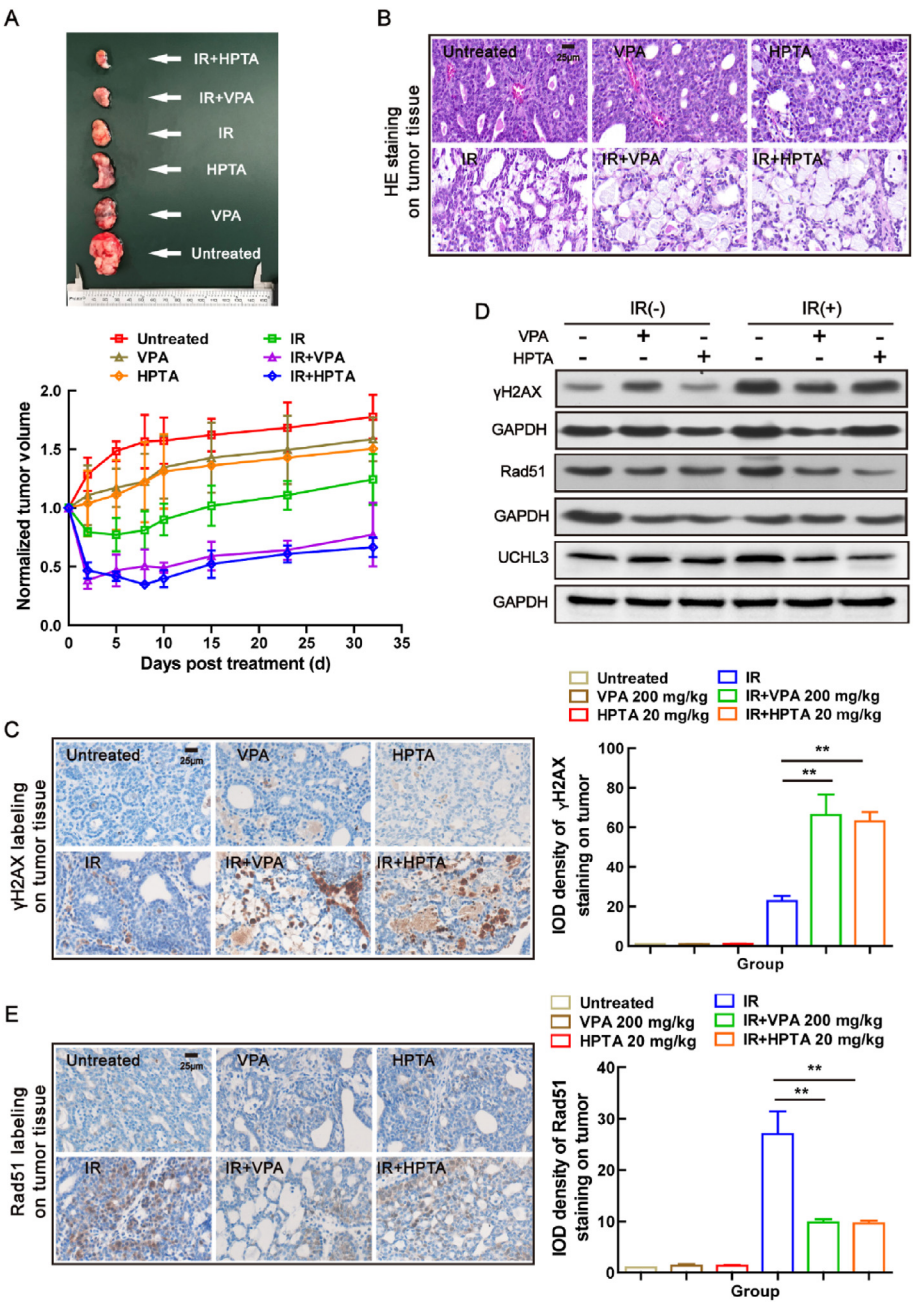

Fig. 5. 2-Hexyl-4-pentynoic acid (HPTA) exhibits radiosensitizing properties to ionizing radiation (IR) treatment in 7,12-dimethylbenz-[α]-anthracene (DMBA)-induced breast cancer *in vivo*. A. Tumor volume changes across different groups, normalized by the untreated group ($n = 6$ in each group). B. Morphological changes in tumors were evaluated by hematoxylin–eosin staining. C. γH2AX expression *in situ* was detected by immunohistochemical staining, and integrated optical density was analyzed. D. γH2AX, Rad51, and UCHL3 protein levels were detected by immunoblotting using whole lysates of treated tumor tissues. E. Rad51 expression *in situ* was detected by immunohistochemical staining, and integrated optical density was analyzed. Each data point in the graph represents data collected from three independent experiments (mean ± SD). $^{*}P < 0.05$, $^{**}P < 0.01$.

observed through immunoblotting (Fig. 5D). Breast cancer-derived primary culture cells were used to further validate our findings(Fig. S5E). γH2AX and 53BP1 foci formation in these primary culture cells (Fig. S5F) supported the earlier findings of HPTA-induced DSB accumulation. With regard to repair proteins, both immunohistochemistry and immunoblotting indicated that Rad51 levels in the combined treatment group were significantly lower than those in the IR alone group ($P<0.01$; Fig. 5D and E). Importantly, UCHL3 expression was significantly downregulated in the combined treatment group ($P<0.01$; Fig. 5E). Based on *in vivo* experiment results, we concluded that low-dose HPTA exhibits radiosensitizing effects associated with increased DSBs *via* the HR-associated UCHL3–Rad51 pathway.

4. Discussion

In this study, we found that 15 μmol/L HPTA has a radiosensitizing effect on breast tumor cells *in vitro* and *in vivo*. This is accomplished by targeting the UCHL3-dependent Rad51 deubiquitination pathway, which modulates HR-mediated DNA DSB repair, leading to increased sensitivity to IR (Fig. 6). Our finding showed that HPTA serves as a potential radiosensitizer for breast cancer by regulating UCHL3-dependent Rad51 deubiquitination.

4.1. New role of HPTA, a highly effective radiosensitizer

Since the discovery of the antitumor and radiosensitizing effects of VPA,[6, 7, 10, 11] interest has grown in exploring the potential of VPA for the clinical usage due to its ready availability (listed as an essential medicine by the World Health Organization), low cost, and long history of therapeutic use in epilepsy. However, adverse events of VPA are dose-dependent, and the higher dose required for its radiosensitizing effects in experimental studies have limited its clinical potential. There is now renewed interest in VPA derivatives, such as HPTA, which are potentially safer and as effective as VPA in terms of their radiosensitizing effects. We

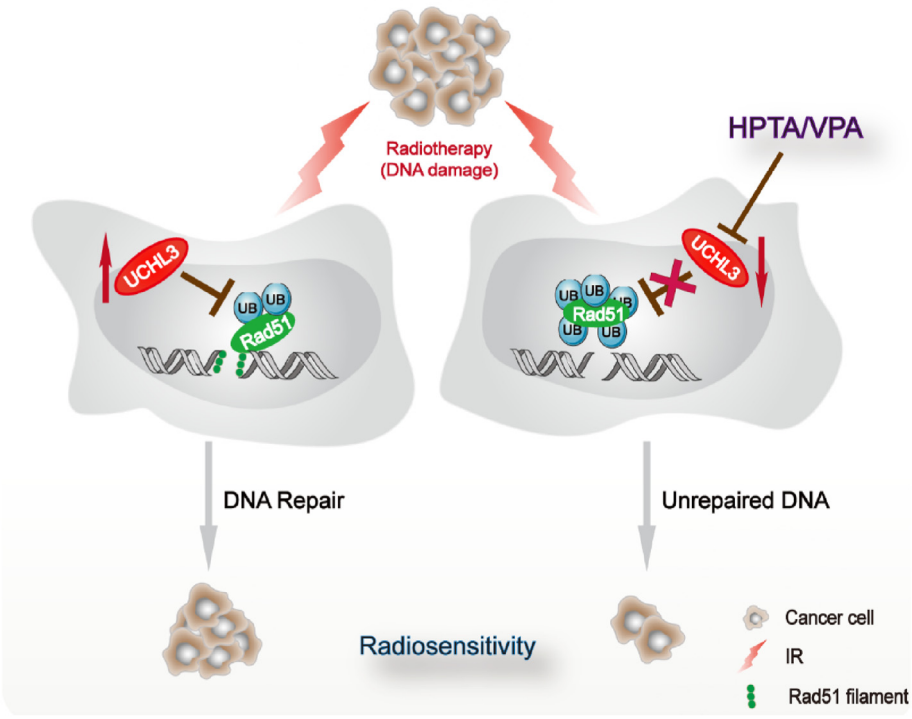

Fig. 6. Molecular model for radiosensitization of breast tumors by 2-hexyl-4-pentynoic acid (HPTA)/valproic acid (VPA). Inhibition of homologous recombination (HR)-mediated DNA double-strand break (DSB) damage repair by the ubiquitin carboxyl-terminal hydrolase L3 (UCHL3)-dependent Rad51 deubiquitination pathway.

propose that HPTA can serve as a promising radiosensitizer for breast cancer. Notably, our *in vitro* and *in vivo* working model results indicate that a lower dose of HPTA (15 μmol/L) is as effective as the higher dose (500 μmol/L) of VPA, suggesting that HPTA is more efficacious than VPA.

Furthermore, we found that HPTA exhibited antitumor effects in the DMBA-induced breast cancer rat model. Our tumor growth experiment and hematoxylin–eosin staining findings revealed, for the first time, that HPTA alone can inhibit tumor growth and exert antitumor effects. A previous study reported similar observations with VPA.[29] In contrast to the results of our cellular-level experiments, an obvious effect of HPTA treatment alone on tumor cell viability was not observed; in addition, an increase in the DNA DSB marker γH2AX in our animal model was not observed, either. Altogether, these results suggest that HPTA exerts antitumor effects *in vivo* through a mechanism distinct from IR. Further investigations are warranted.

4.2. Radiosensitizing effects of HPTA and HR/NHEJ mechanism

IR is known to induce DNA DSBs in cancer cells. However, the robust functioning of HR evidently contributes to treatment resistance and therapy failure.[30] On the contrary, HR deficiency often triggers genomic instability, increasing cancer susceptibility.[31] Therefore, targeting the HR repair pathway holds potential to enhance the sensitivity of cancer cells to IR treatment.

Rad51 is one of the most important proteins in HR, as it participates in Rad51-ssDNA filament-dependent homology search and synaptic complex formation, both of which are critical steps in HR. Disrupting HR repair by regulating Rad51 protein expression represents a promising approach in cancer therapy.[32] In this study, we demonstrated that HPTA has the capability to inhibit Rad51 protein expression, thereby affecting HR function and exerting its radiosensitizing effect *via* the aforementioned pathway.

The initial stages of HR repair involves the recognition of DNA damage site and modification of end resection. Some studies have indicated that BRCA1, existing as a heterodimer with BRCA1-associated RING domain-1, participates in the HR repair process through the DNA end resection pathway.[33] The inhibition or absence of BRCA1 function leads to impaired HR repair as well as increased sensitivity to DNA damage.[34] In our cellular model, HPTA was found to inhibit BRCA1 protein expression, hindering the initiation phase of HR repair. How HPTA affects the early repair processes of BRCA1-mediated HR function demands further exploration.

NHEJ, another mode of DNA DSB repair, primarily involves the direct ligation of DSB ends by DNA ligase, with the assistance of Ku70/Ku80 and DNA-PKcs. This process involves the recruitment of recombinase Artemis to DSBs ends, which, in turn, recruits the XRCC4/DNA ligase IV/XLF complex to promote DSB end joining.[35] We found that HPTA inhibits NHEJ repair but does not impact major proteins (Ku70/Ku80, DNA-PKcs). Thus, we hypothesize that HPTA affects other proteins associated with the NHEJ pathway; further studies are warranted.

4.3. HPTA-mediated radiosensitization is associated with UCHL3-Rad51 deubiquitination

We observed that HPTA results in a further reduction in Rad51 protein levels in tumor cells upon IR exposure, accompanied by an increase in Rad51 protein ubiquitination level. This suggests that Rad51 inhibition by HPTA is mediated through protein ubiquitination. Further investigation revealed that HPTA regulates Rad51 protein ubiquitination by inhibiting UCHL3 expression.

Although it remains unknown whether HPTA directly inhibits UCHL3, a previous study indicated that in response to DNA damage, ATM can phosphorylate and activate UCHL3.[27] It has also been reported that VPA and fludarabine reduce Akt and ATM total protein and phosphorylation levels.[36] Therefore, it is plausible that HPTA, as a VPA derivative, directly inhibits UCHL3 activation by inhibiting ATM protein expression. Further studies are warranted on this topic.

Funding

This work was supported by grants from Zhejiang Provincial Natural Science Foundation of China (LQ23H14003), National Natural Science Foundation of China (81472800, 82173460), Department of Science and Technology of Shandong Province (2019GSF108083), and Zhejiang Provincial Postdoctoral Scientific Research Project Funding (ZJ2022076), China.

Ethics

This study did not involve human participants, human data, or human tissue. All rat experiments were approved and conducted in accordance with the national standards on animal care and approved by the Shandong University Human and Animal Ethics Research Committee (81472800).

Declaration of conflicting interest

None.

Appendix A. Supplementary data

Supplementary data to this article can be found online at https://doi.org/10.1016/j.radmp.2023.10.003.

References

1. Rutqvist LE, Rose C, Cavallin-Ståhl E. A systematic overview of radiation therapy effects in breast cancer. *Acta Oncol*. 2003;42(5-6):532–545. https://doi.org/10.1080/02841860310014444.
2. McGale P, Darby SC, Hall P, et al. Incidence of heart disease in 35,000 women treated with radiotherapy for breast cancer in Denmark and Sweden. *Radiother Oncol*. 2011;100(2):167–175. https://doi.org/10.1016/j.radonc.2011.06.016.
3. Bolden JE, Peart MJ, Johnstone RW. Anticancer activities of histone deacetylase inhibitors. *Nat Rev Drug Discov*. 2006;5(9):769–784. https://doi.org/10.1038/nrd2133.
4. Robert T, Vanoli F, Chiolo I, et al. HDACs link the DNA damage response, processing of double-strand breaks and autophagy. *Nature*. 2011;471(7336):74–79. https://doi.org/10.1038/nature09803.
5. Shubassi G, Robert T, Vanoli F, et al. Acetylation: a novel link between double-strand break repair and autophagy. *Cancer Res*. 2012;72(6):1332–1335. https://doi.org/10.1158/0008-5472.CAN-11-3172.
6. Chen X, Wong P, Radany E, et al. HDAC inhibitor, valproic acid, induces p53-dependent radiosensitization of colon cancer cells. *Cancer Biother Radiopharm*. 2009;24(6):689–699. https://doi.org/10.1089/cbr.2009.0629.
7. Entin-Meer M, Rephaeli A, Yang X, et al. Butyric acid prodrugs are histone deacetylase inhibitors that show antineoplastic activity and radiosensitizing capacity in the treatment of malignant gliomas. *Mol Cancer Therapeut*. 2005;4(12):1952–1961. https://doi.org/10.1158/1535-7163.MCT-05-0087.
8. Thotala D, Karvas RM, Engelbach JA, et al. Valproic acid enhances the efficacy of radiation therapy by protecting normal hippocampal neurons and sensitizing malignant glioblastoma cells. *Oncotarget*. 2015;6(33):35004–35022. https://doi.org/10.18632/oncotarget.5253.
9. Zhang H, Zhang W, Zhou Y, et al. Dual functional mesoporous silicon nanoparticles enhance the radiosensitivity of VPA in glioblastoma. *Transl Oncol*. 2017;10(2):229–240. https://doi.org/10.1016/j.tranon.2016.12.011.
10. Liu G, Wang H, Zhang F, et al. The effect of VPA on increasing radiosensitivity in osteosarcoma cells and primary-culture cells from chemical carcinogen-induced breast cancer in rats. *Int J Mol Sci*. 2017;18(5):1027. https://doi.org/10.3390/ijms18051027.
11. Luo Y, Wang H, Zhao X, et al. Valproic acid causes radiosensitivity of breast cancer cells *via* disrupting the DNA repair pathway. *Toxicol Res*. 2016;5(3):859–870. https://doi.org/10.1039/c5tx00476d.
12. Eikel D, Lampen A, Nau H. Teratogenic effects mediated by inhibition of histone deacetylases: evidence from quantitative structure activity relationships of 20 valproic acid derivatives. *Chem Res Toxicol*. 2006;19(2):272–278. https://doi.org/10.1021/tx0502241.
13. Leng Y, Marinova Z, Reis-Fernandes MA, et al. Potent neuroprotective effects of novel structural derivatives of valproic acid: potential roles of HDAC inhibition and HSP70 induction. *Neurosci Lett*. 2010;476(3):127–132. https://doi.org/10.1016/j.neulet.2010.04.013.
14. Lampen A, Siehler S, Ellerbeck U, et al. New molecular bioassays for the estimation of the teratogenic potency of valproic acid derivatives in vitro: activation of the peroxisomal proliferator-activated receptor (PPARdelta). *Toxicol Appl Pharmacol*. 1999;160(3):238–249. https://doi.org/10.1006/taap.1999.8770.
15. Ding W, Lim D, Wang Z, et al. 2-hexyl-4-pentynoic acid, a potential therapeutic for breast carcinoma by influencing RPA2 hyperphosphorylation-mediated DNA repair. *DNA Repair*. 2020;95:102940. https://doi.org/10.1016/j.dnarep.2020.102940.
16. Liu G, Lim D, Cai Z, et al. The valproate mediates radio-bidirectional regulation through RFWD3-dependent ubiquitination on Rad51. *Front Oncol*. 2021;11:646256. https://doi.org/10.3389/fonc.2021.646256.
17. Luo K, Li L, Li Y, et al. A phosphorylation-deubiquitination cascade regulates the BRCA2-RAD51 axis in homologous recombination. *Genes Dev*. 2016;30(23):2581–2595. https://doi.org/10.1101/gad.289439.116.
18. Song Z, Tu X, Zhou Q, et al. A novel UCHL3 inhibitor, perifosine, enhances PARP inhibitor cytotoxicity through inhibition of homologous recombination-mediated DNA double strand break repair. *Cell Death Dis*. 2019;10(6):398. https://doi.org/10.1038/s41419-019-1628-8.
19. Feng Z, Scott SP, Bussen W, et al. Rad52 inactivation is synthetically lethal with BRCA2 deficiency. *Proc Natl Acad Sci U S A*. 2011;108(2):686–691. https://doi.org/10.1073/pnas.1010959107.
20. Feng Z, Zhang J. A dual role of BRCA1 in two distinct homologous recombination mediated repair in response to replication arrest. *Nucleic Acids Res*. 2012;40(2):726–738. https://doi.org/10.1093/nar/gkr748.
21. Gunn A, Stark JM. I-SceI-based assays to examine distinct repair outcomes of mammalian chromosomal double strand breaks. *Methods Mol Biol*. 2012;920:379–391. https://doi.org/10.1007/978-1-61779-998-3_27.
22. Peng J, Cai Z, Zhao R, et al. The intervention of valproic acid on the tumorigenesis induced by an environmental carcinogen of PAHs. *Toxicol Res*. 2020;9(5):609–621. https://doi.org/10.1093/toxres/tfaa069.
23. Dong C, Zhang F, Luo Y, et al. p53 suppresses hyper-recombination by modulating BRCA1 function. *DNA Repair*. 2015;33:60–69. https://doi.org/10.1016/j.dnarep.2015.06.005.
24. Tian Y, Liu G, Wang H, et al. Valproic acid sensitizes breast cancer cells to hydroxyurea through inhibiting RPA2 hyperphosphorylation-mediated DNA repair pathway. *DNA Repair*. 2017;58:1–12. https://doi.org/10.1016/j.dnarep.2017.08.002.
25. Budke B, Logan HL, Kalin JH, et al. RI-1: a chemical inhibitor of RAD51 that disrupts homologous recombination in human cells. *Nucleic Acids Res*. 2012;40(15):7347–7357. https://doi.org/10.1093/nar/gks353.
26. Wu L, Shao L, Li M, et al. BMS-345541 sensitizes MCF-7 breast cancer cells to ionizing radiation by selective inhibition of homologous recombinational repair of DNA double-strand breaks. *Radiat Res*. 2013;179(2):160–170. https://doi.org/10.1667/RR3034.1.
27. Luo K, Li L, Li Y, et al. A phosphorylation-deubiquitination cascade regulates the BRCA2-RAD51 axis in homologous recombination. *Genes Dev*. 2016;30(23):2581–2595. https://doi.org/10.1101/gad.289439.116.
28. Krug D, Baumann R, Budach W, et al. Current controversies in radiotherapy for breast cancer. *Radiat Oncol*. 2017;12(1):25. https://doi.org/10.1186/s13014-017-0766-3.
29. Sun J, Piao J, Li N, et al. Valproic acid targets HDAC1/2 and HDAC1/PTEN/Akt signalling to inhibit cell proliferation via the induction of autophagy in gastric cancer. *FEBS J*. 2020;287(10):2118–2133. https://doi.org/10.1111/febs.15122.
30. Parmar K, Kochupurakkal BS, Lazaro JB, et al. The CHK1 inhibitor prexasertib exhibits monotherapy activity in high-grade serous ovarian cancer models and sensitizes to PARP inhibition. *Clin Cancer Res*. 2019;25(20):6127–6140. https://doi.org/10.1158/1078-0432.CCR-19-0448.
31. Ceccaldi R, Liu JC, Amunugama R, et al. Homologous-recombination-deficient tumours are dependent on Polθ-mediated repair. *Nature*. 2015;518(7538):258–262. https://doi.org/10.1038/nature14184.
32. Ward A, Khanna KK, Wiegmans AP. Targeting homologous recombination, new pre-clinical and clinical therapeutic combinations inhibiting RAD51. *Cancer Treat Rev*. 2015;41(1):35–45. https://doi.org/10.1016/j.ctrv.2014.10.006.
33. Wang Y, Krais JJ, Bernhardy AJ, et al. RING domain-deficient BRCA1 promotes PARP inhibitor and platinum resistance. *J Clin Invest*. 2016;126(8):3145–3157. https://doi.org/10.1172/JCI87033.
34. Krais JJ, Johnson N. BRCA1 mutations in cancer: coordinating deficiencies in homologous recombination with tumorigenesis. *Cancer Res*. 2020;80(21):4601–4609. https://doi.org/10.1158/0008-5472.CAN-20-1830.
35. Ciccia A, Elledge SJ. The DNA damage response: making it safe to play with knives. *Mol Cell*. 2010;40(2):179–204. https://doi.org/10.1016/j.molcel.2010.09.019.
36. Yoon JY, Ishdorj G, Graham BA, et al. Valproic acid enhances fludarabine-induced apoptosis mediated by ROS and involving decreased AKT and ATM activation in B-cell-lymphoid neoplastic cells. *Apoptosis*. 2014;19(1):191–200. https://doi.org/10.1007/s10495-013-0906-7.